

# Multiple-scale neuroendocrine signals connect brain and pituitary hormone rhythms

Romanò, Nicola; Guillou, Anne; Hodson, David J.; Martin, Agnes O; Mollard, Patrice

DOI:

[10.1073/pnas.1616864114](https://doi.org/10.1073/pnas.1616864114)

License:

None: All rights reserved

*Document Version*

Peer reviewed version

*Citation for published version (Harvard):*

Romanò, N, Guillou, A, Hodson, DJ, Martin, AO & Mollard, P 2017, 'Multiple-scale neuroendocrine signals connect brain and pituitary hormone rhythms', *National Academy of Sciences. Proceedings*, vol. 114, no. 9, pp. 2379–2382. <https://doi.org/10.1073/pnas.1616864114>

[Link to publication on Research at Birmingham portal](#)

## General rights

Unless a licence is specified above, all rights (including copyright and moral rights) in this document are retained by the authors and/or the copyright holders. The express permission of the copyright holder must be obtained for any use of this material other than for purposes permitted by law.

- Users may freely distribute the URL that is used to identify this publication.
- Users may download and/or print one copy of the publication from the University of Birmingham research portal for the purpose of private study or non-commercial research.
- User may use extracts from the document in line with the concept of 'fair dealing' under the Copyright, Designs and Patents Act 1988 (?)
- Users may not further distribute the material nor use it for the purposes of commercial gain.

Where a licence is displayed above, please note the terms and conditions of the licence govern your use of this document.

When citing, please reference the published version.

## Take down policy

While the University of Birmingham exercises care and attention in making items available there are rare occasions when an item has been uploaded in error or has been deemed to be commercially or otherwise sensitive.

If you believe that this is the case for this document, please contact [UBIRA@lists.bham.ac.uk](mailto:UBIRA@lists.bham.ac.uk) providing details and we will remove access to the work immediately and investigate.

## Supporting information

Romanò et al.

### SI Materials and Methods

#### Animals

C57/BL6 virgin female mice were housed under a 12 hour light-dark cycle (lights on at 0900), with *ad libitum* access to water and food *ad libitum*. The estrus cycle of the animals was checked daily between 9 and 10 AM through examination of vaginal cytology. Pregnancy and lactation were induced using standard timed mating procedures. All animal procedures were approved by the local ethical committee under agreement CEEA-LR-12185 according to EU Directive 2010/63/EU. Since this study included only one experimental group of animals, no randomization or blinding was required.

#### Fabrication of carbon fiber microelectrodes and optic fibers

A single thread of carbon fiber (30 µm diameter, World Precision Instruments) was inserted under a stereo-microscope through the opening of a flexible silica capillary (Polymicro Technologies™ 40 µm ID, 150 µm OD, Molex), leaving approximately 500µm protruding from each extremity. A gold-plated pin (World Precision instruments) was then fixed to one end using conductive glue (Carbon-epoxy, World Precision Instruments). The carbon epoxy was allowed to cure for 2 hours at 75 °C, then cyanoacrylate glue was used to seal the capillary at the detecting end, taking care not to cover the tip of the carbon fiber. A Nafion™ coating was applied by dipping the exposed fiber in Nafion™ perfluorinated solution (Sigma-Aldrich), while applying a 3 V potential to the microelectrode. This strongly reduces the non-specific signal derived from the oxidation of ascorbate molecules (24). Before implantation, electrodes were calibrated *in vitro* using standard solutions of DA, and those that did not respond to DA (*e.g.* because of faulty contact between the pin and the fiber, broken fiber *etc.*) were discarded.

#### Implantation of microelectrodes

Mice were anesthetized with 10 µl/g body weight of a mix of 1 % ketamine and 0.1 % xylazine in 0.9 % NaCl. The head of the mouse was then attached to a stereotaxic frame and sterilized with 10 % betadine. A sagittal incision was made through the skin of the cranium to expose the sagittal suture, before craniotomy using a dental burr. Three jeweler's screws (Plastics One) were fixed to the skull to improve stability of the head-cap, and a ground pin attached to one of them. A support guide cannula (Plastics One) was then inserted 1.5 mm above the median eminence, and fixed to the skull with Dentalon dental acrylic (Phymep). A carbon fiber microelectrode was then slowly passed through the guide cannula, so that its tip reached the median eminence at the stereotaxic coordinates (relative to Bregma) -1.3 mm rostro-caudal; 0 mm medio-lateral; 6.1 mm ventral. The implant was finally blocked with dental acrylic and the mouse left to recover for at least a week before initiating the recording. Post-operative analgesia was provided using i.m. injection of the non-steroidal anti-inflammatory (NSAID) ketoprofen. A similar procedure was used for double implants, except that fibers were fixed to a double cannula, with 500 µm spacing between the two guides. The gold-plated pins were isolated using silicone tubing to prevent electrical contact between the two channels and a drop of dental wax was used to isolate the two pins.

### **In vivo amperometry**

Mice were transferred to recording cages, connected to an electrical swivel (Plastics One) to allow for free movement. A Faraday cage was used to limit electrical noise. Food and water were provided *ad libitum*. Recordings were started at least two days following transfer to the recording cage to allow the mouse to habituate to the new environment. Throughout, carbon fiber microelectrodes were held at 700 mV using a HEKA EPC10 amplifier, as previously reported<sup>2</sup> to detect secretion of DA, and oxidation currents were recorded at 1 kHz. Animals for which no electrical signal was detected or those where the electrode was found to be implanted away from the ME at the end of the experiment were discarded from the analysis.

### **Prolactin measurements**

Repeated tail blood microsampling was performed during one-hour sessions in the late afternoon, when the density of DA signal was higher. Briefly, 4  $\mu$ l blood samples were withdrawn from the tail vein every 5 minutes, and diluted with 96  $\mu$ l PBS-Tween 20 before storage at -80 °C pending analysis. Prolactin concentrations were measured using a home-made ELISA, as previously reported (10). In some experiments, i.p. injection of ovine PRL (Sigma) was performed during tail-tip blood sampling (Fig. S2).

### **Data analysis**

Raw data from PatchMaster (HEKA) files were imported into IGOR Pro (Wavemetrics) and a threshold algorithm used to identify peaks. Peaks were defined as having intensity greater than 10 standard deviations from baseline noise, with a minimum width of at least 50 ms. The times and shapes of the detected peaks were then exported to flat text files and further analyzed using R software. Event distribution was studied using standard techniques for the analysis of point-processes, such as analysis of the inter-spike intervals. Classification of DA release events was performed using k-means clustering. The width, amplitude, AUC and 5 quantiles of the peak shape were used as classifiers for clustering.

Repeated temporal patterns were found by first determining all  $n$ -long sequences of events ( $3 \leq n \leq 10$ ), with a maximum total length of 5 hours, taking into account the cluster to which each group belonged to. Patterns formed by the same series of events (same sequence of clusters, and with the same IEs, with a tolerance of  $\pm 15$  % for each IEI), were grouped together. Groups with less than 5 sequences were not considered. The same process was repeated on 1,000 bootstrap samples of the time series, obtained by randomly shuffling the IEI. The 95<sup>th</sup> centile of the distribution of the maximum number of repeated patterns found in a group of each bootstrap sample was used as the limit at which results were deemed statistically significant. As expected, this limit is higher for shorter sequences (Fig. S4A).

The relation between PRL levels and DA events was calculated by averaging the linearly interpolated PRL levels measured around each detected DA event. The levels were then normalized between 0 and 1 and averaged between recordings. This generated the “mean” PRL response to a DA release event shown in Figure 1F, demonstrating the inverse relationship between DA and PRL.

For double recordings, cross-density histograms were generated by plotting the histogram of the IEI between the events recorded by the two electrodes, as previously reported (9, 25). Furthermore, a similarity index (cosine similarity, defined as  $(A \cdot B) / (||A|| * ||B||)$ , where A and B are the vectors of events at the two electrodes) was used to determine whether the “loose synchronization” of the events in the two recordings was higher than that expected by chance. The similarity index was calculated for each recording, and for 1000 bootstrap samples in which the IEIs from a single electrode were randomly shuffled. In all cases, the real data had similarity above the 95% confidence interval of the bootstrapped data.

Estrus cycle data was analyzed using a mixed effects model. The cycle stage and the time of the day (in 4 hours blocks) were used as fixed effects, the animal as a random effect. Tukey’s all-pair comparisons post-hoc analysis was then performed to compare the effect of the stage of the cycle.

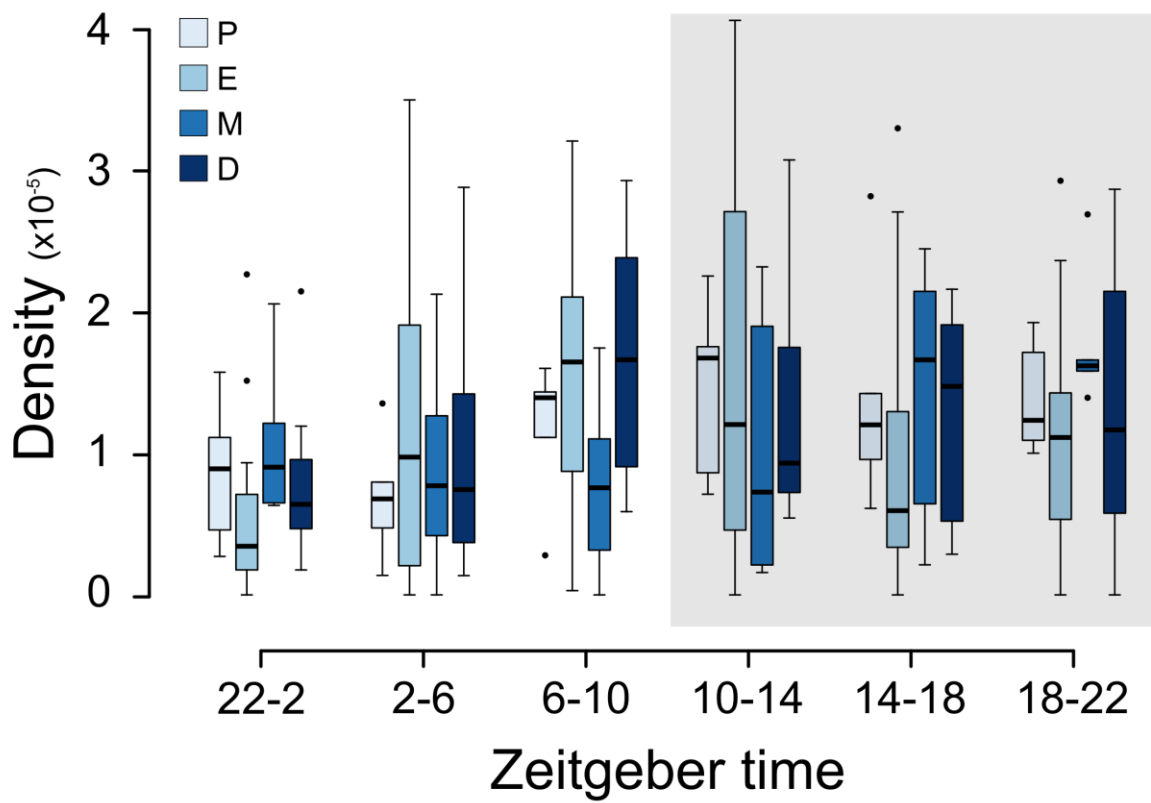


**Fig. S1.** Average frequency of DA release events during the different stages of the estrus cycle (M, metestrus; D, diestrus; P, proestrus, E, estrus) ( $n = 5$  female mice, *shaded area is lights-out*). No statistical difference between the different days of the cycle was detected ( $p > 0.05$ , mixed effects model). Individual data points which are outside of the interquartile range (indicated by bars) are shown as dots.

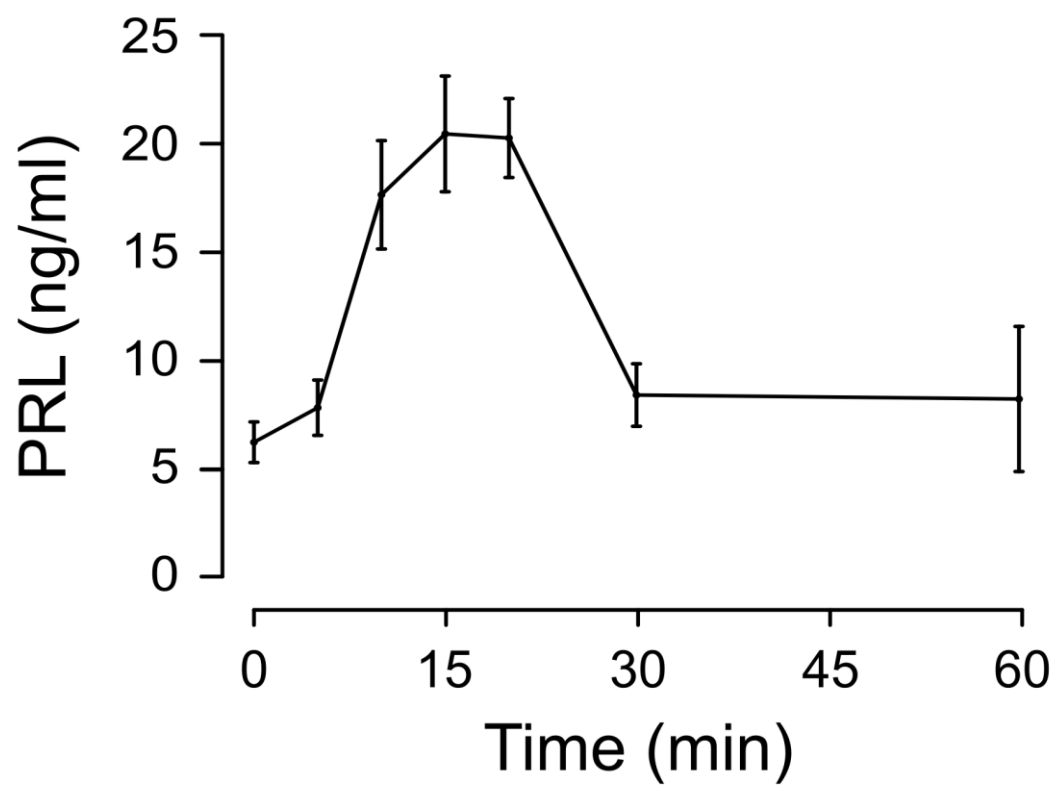


**Fig. S2.** Levels of PRL detected after i.p. injection of 1 µg oPRL in B6 female mice (n = 6, mean ± SEM).

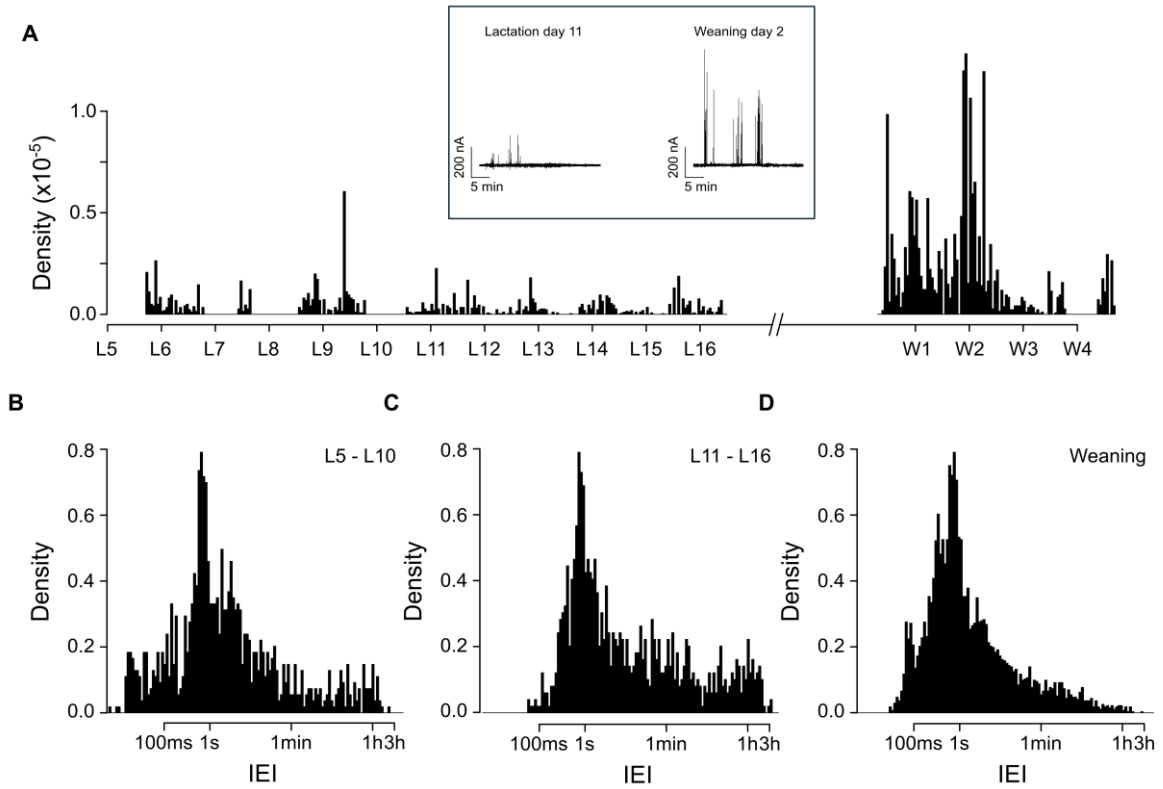


**Fig. S3.** (A) Density of secretory events in a mouse recorded during lactation (days 6 to 16) and weaning (day 1 to 4) ( $n = 2$ ). Insets show examples of the raw signal. (B-D) Distribution of IEIs during different phases of the recording in A.

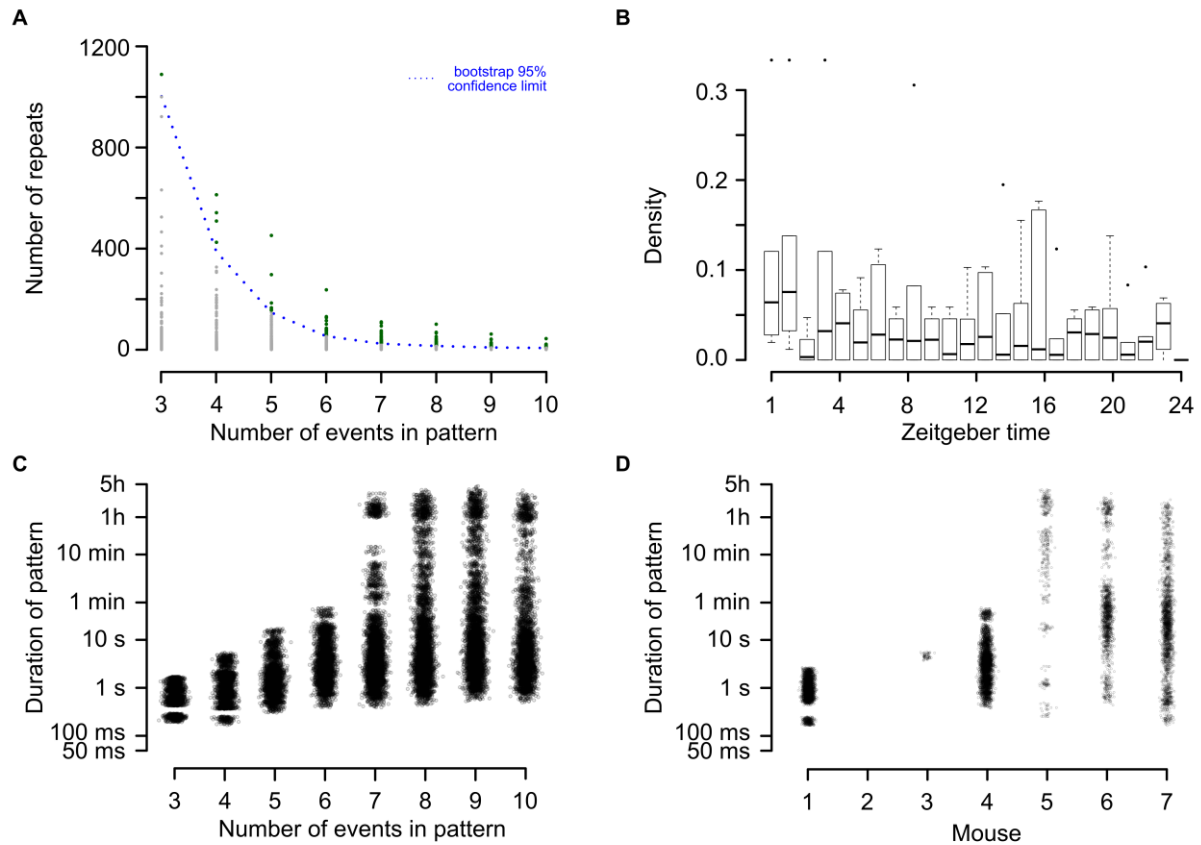


**Fig. S4.** Properties of release patterns. (A) Choice of statistically significant patterns. Each recording was analyzed for  $n$ -event long ( $3 \leq n \leq 10$ ) patterns, repeated at least 5 times. The number of occurrences of each pattern are plotted against  $n$ , each dot representing one temporal pattern. The same procedure was repeated on 1000 computer-generated sequences, with the same number of events, same distribution of IEI, and same proportion of different classes. A 95 % confidence limit (blue dotted line) was then calculated for the distribution of the maximum number of repeats in the bootstrap samples. Patterns repeated a greater number of times than the bootstrap limit are indicated in green, and are considered to be occurring with a higher-than-chance probability. (B) Distribution of temporal patterns during the day ( $n = 7$  mice). (C) Duration of statistically significant temporal patterns in the recording from mouse 4, in relation to the number of events in the pattern. (D) Duration of statistically significant 6-event long temporal patterns in 7 different mice.